

# Waves and Magnetism in the Solar Atmosphere (WAMIS)

L. Strachan<sup>1,7</sup>, Y.-K. Ko<sup>1</sup>, J. D. Moses<sup>1</sup>, J. M. Laming<sup>1</sup>, F. Auchere<sup>2</sup>, R. Casini<sup>3</sup>, S. Fineschi<sup>4</sup>, S. Gibson<sup>3</sup>, M. Knoelker<sup>3</sup>, C. Korendyke<sup>1</sup>, S. McIntosh<sup>3</sup>, M. Romoli<sup>5</sup>, J. Rybak<sup>6</sup>, D. Socker<sup>1</sup>, S. Tomczyk<sup>3</sup>, A. Vourlidas<sup>1,8</sup>, Q. Wu<sup>3</sup>

<sup>1</sup>Naval Research Laboratory, <sup>2</sup>Institut d'Astrophysique Spatiale, <sup>3</sup>High Altitude Observatory, <sup>4</sup>INAF-Astrophysical Observatory of Turin, <sup>5</sup>University of Florence, <sup>6</sup>Astronomical Institute of the Slovak, Academy of Sciences, <sup>7</sup>also Smithsonian Research Associate, <sup>8</sup>now at Johns Hopkins Univ./APL

## 1. What is WAMIS?

WAMIS is the **W**aves **A**nd **M**agnetism In the Solar Atmosphere mission proposed for the NASA Low Cost Access to Space program. It is designed to make direct solar coronal measurements of not only the strength and orientation of the magnetic field but also the signatures of wave motions in order to better understand coronal structure, solar activity and the role of MHD waves in heating and accelerating the solar wind.

WAMIS will take advantage of greatly improved infrared (InGaAs) detectors, forward models, advanced diagnostic tools and inversion codes to obtain a breakthrough in the measurement of coronal magnetic fields and in the understanding of the interaction of these fields with space plasmas. This will be achieved with a high altitude balloon borne payload consisting of a coronagraph with an IR spectro-polarimeter focal plane assembly. The balloon platform provides minimum atmospheric absorption and scattering at the IR wavelengths in which these observations are made.

This work is supported by the Office of Naval Research and NASA NDPR NNG13WF951.

## 2. Science Objectives

### I. What determines the magnetic structure of the corona?

- Global structure of the coronal magnetic field
- Evolution and interaction between closed and open field regions
- Distinction between fast and slow solar wind via propagating wave properties

### II. How do flux ropes form and evolve, and how are they related to CMEs?

- Relationship between coronal loops, flux rope formation and CME eruption
- Magnetic structure and physical properties in prominence and prominence cavity

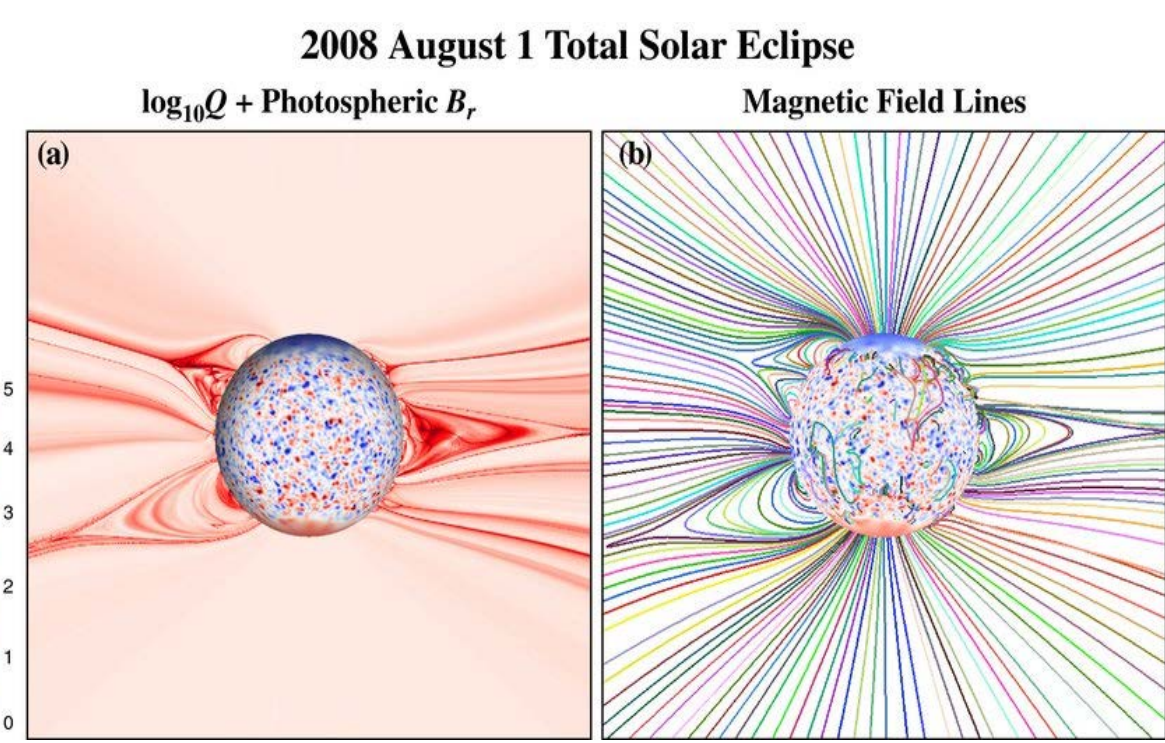
### III. Where do CME-associated shocks form?

- Observing shock formation in action in relation to the ambient coronal properties
- Measurements of shock strength, shock obliquity, and associated waves

### IV. How is energy stored and released by reconnection in flares and CMEs?

- Measurement of non-potential magnetic field and calculation of magnetic free energy
- Formation and properties of post-CME current sheet during CME eruption

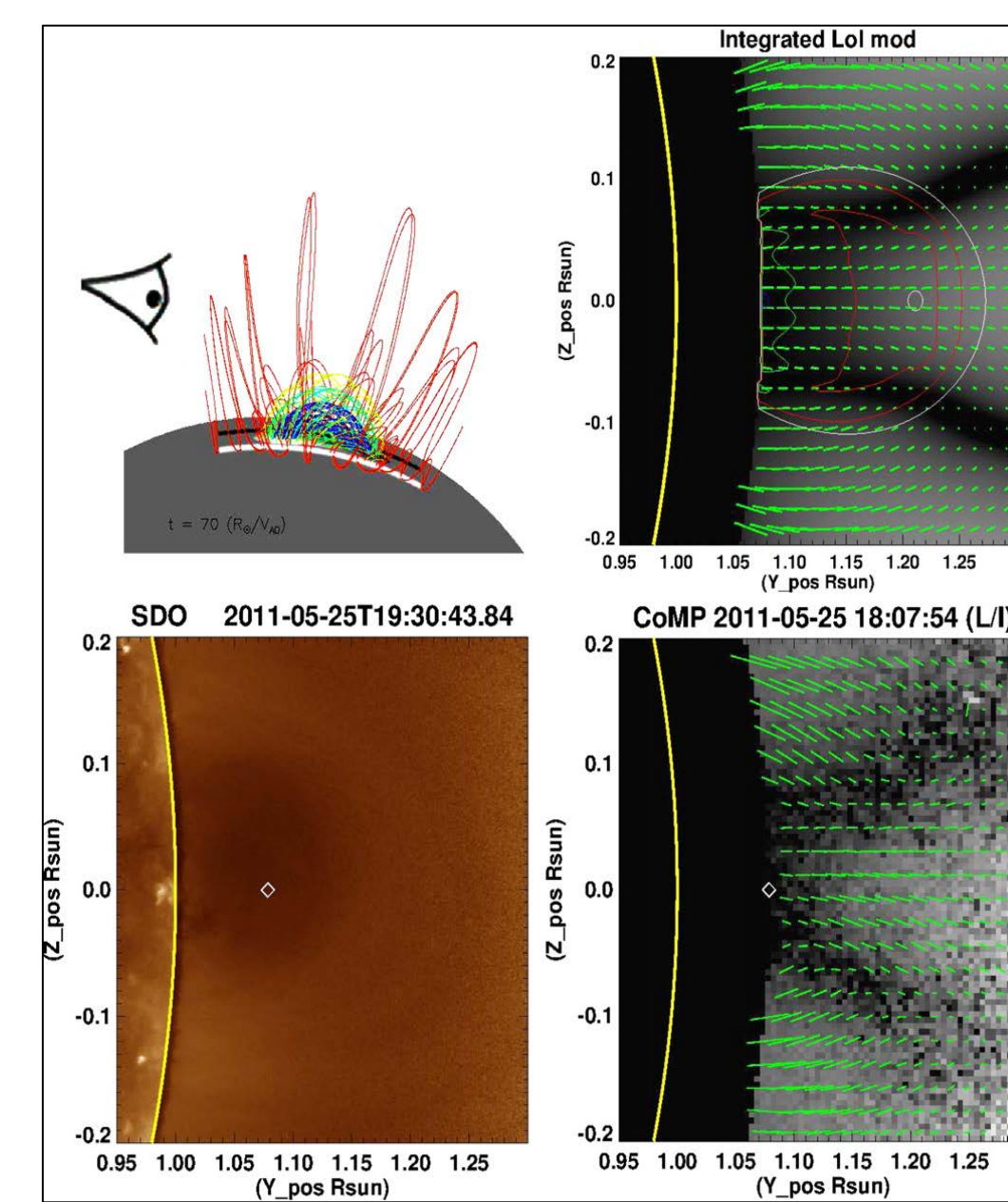
## Science Obj. I: Coronal Magnetic Structure



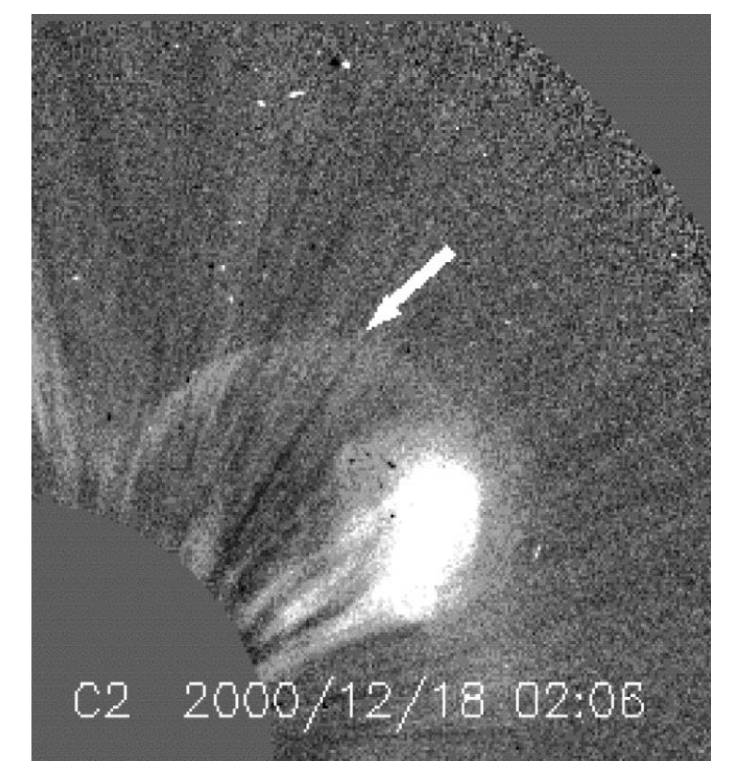
(a) Plot of squashing factor  $Q$  on log scale for 2008 August 1 eclipse.  $Q \sim (\text{gradient of magnetic connectivity})^2$  and high  $Q$  indicates a quasi-separatrix layer ( $Q \rightarrow \infty$  indicates a true separatrix). (b) Magnetic field lines showing open and closed field, various field line expansions and streamer/pseudostreamer structures. Figure is from Antiochos et al. (2011).

## Science Obj. II: Flux Ropes and CMEs

Coronal prominence cavities, for example as observed by SDO/AIA193Å channel (lower left), are often observed by CoMP to have a characteristic Fe XIII linear polarization signature (lower right; the white diamonds show the center of the cavity). This signature can be explained as arising from an arched magnetic flux rope with axis oriented along the line of sight (e.g., shown here in PoS from 3D simulation of Fan 2010; upper left). When integrated along the line of sight, a combination of linear polarization nulls occurring where the flux rope magnetic field is oriented at the van Vleck angle  $\theta$ , ( $\cos^2\theta=1/3$ ), or where the axial magnetic field is oriented completely out of the PoS, leads to a forward-modeled signal of the same characteristic shape as observed (upper right; the contours show the current density in the simulations). Figure is from Bak-Steslicka et al. (2013).



## Sci. Obj. III: CME Shock Formation



A possible example of a CME shock signature in SOHO/LASCO C2 white light observations on Dec.18, 2000. The white-light structure indicated by the arrow could be the density enhancement from a shock. A pre-event image has been subtracted from this exposure. From Vourlidas et al. (2003).

Table 1. WAMIS Long Duration Balloon (LDB) Instrument Characteristics	
Telescope type	Internally occulted Lyot coronagraph
Objective lens	f/10 singlet, aperture 20cm, focal length 203.3cm
Objective Stray Light	<0.2 $\mu B_{\odot}$ goal 1.2-2.8 $R_{\odot}$
Overall Throughput	$\approx 5\%$
$B_{\odot}$	$9.34 \times 10^6 \text{ erg/cm}^2/\text{s}/\text{sr}/\text{nm}$
Plate Scale	4.5"/pixel low mag. 1.5"/pixel high mag.
Fe XIII (1074.7nm) Count Rate @ 1.1 $R_{\odot}$	$1 \times 10^5$ photons/pixel/sec @ 1.5"/pixel magnification
Detector	Goodrich camera 15 micron pixels, 1280x1024 format
Inner FOV Limit	1.02 $R_{\odot}$
Outer FOV	$\pm 2.8 R_{\odot}$ @ 4.5"/pixel Sun Centered
	1.8 $R_{\odot}$ @ 1.5"/pixel Limb Centered
Primary Lines of Interest	Fe XIII (1074.7, 1079.8 nm) Fe X (637.5 nm) He I (1083.0 nm)
Filter	Tunable Lyot filter, 3.8cm aperture 530 – 1083 nm range
Duration of Continuous Observational Sequence	2 weeks minimum $\geq 4$ week optimum

## 3. Mission Concept Overview

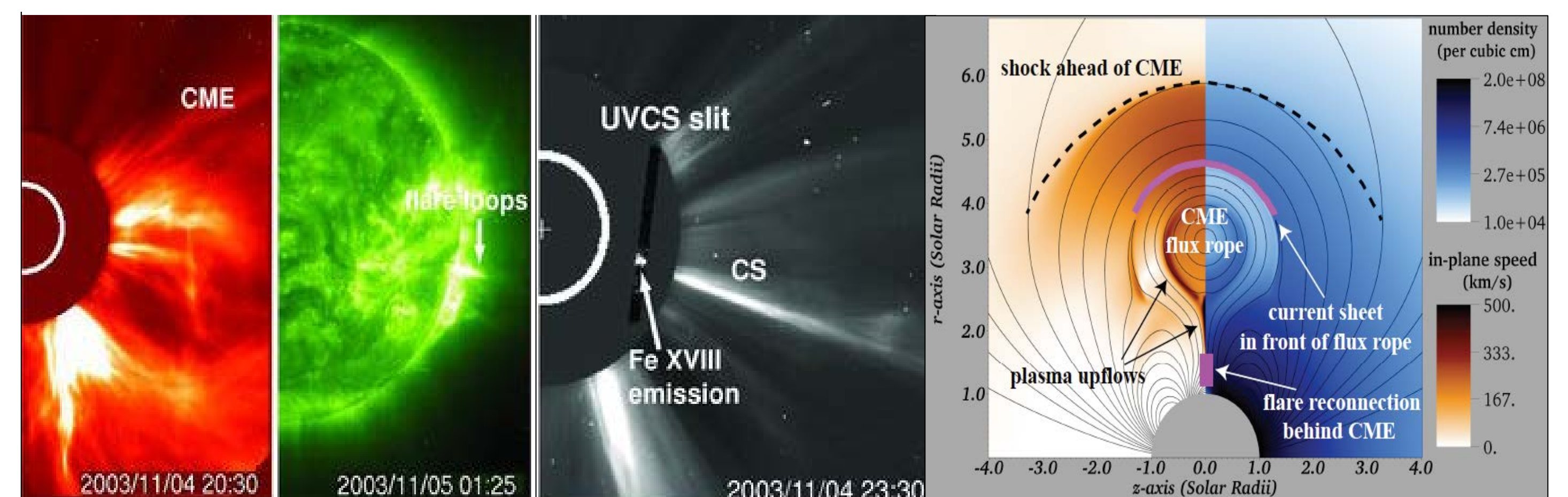
### Why a long duration balloon payload?

- To remove the variability in the sky polarization background
- To improve the stray light levels by reducing the sky brightness background
- To increase the flight duration to at least 2 weeks (1/2 solar rotation) of observations without day-night cycle or weather related interruptions. This provides better temporal resolution and increases the probability for observing transients. This also allows for tomographic reconstruction to separate the 3D structure of the corona from short-term temporal evolution.

## 4. Observational Parameters

The **Observational Requirements** and **Key Observables** are shown in Tables 2 and 3 shown to the right.

## Science Obj. IV: Global Magnetic Storage



A CME with current sheet. Images (left to right) are from SOHO/LASCO (red image), SOHO/EIT  $\lambda 195$  (in green), SOHO/UVCS (slit image marked in the third panel). Fourth image is a simulation of breakout CME (courtesy V. Lukin). This shows the relationship between the erupting CME, the postflare loops, and the post-eruption current sheet, visible to UVCS by Fe XVIII emission. Figure is from Ciaravella & Raymond (2008).

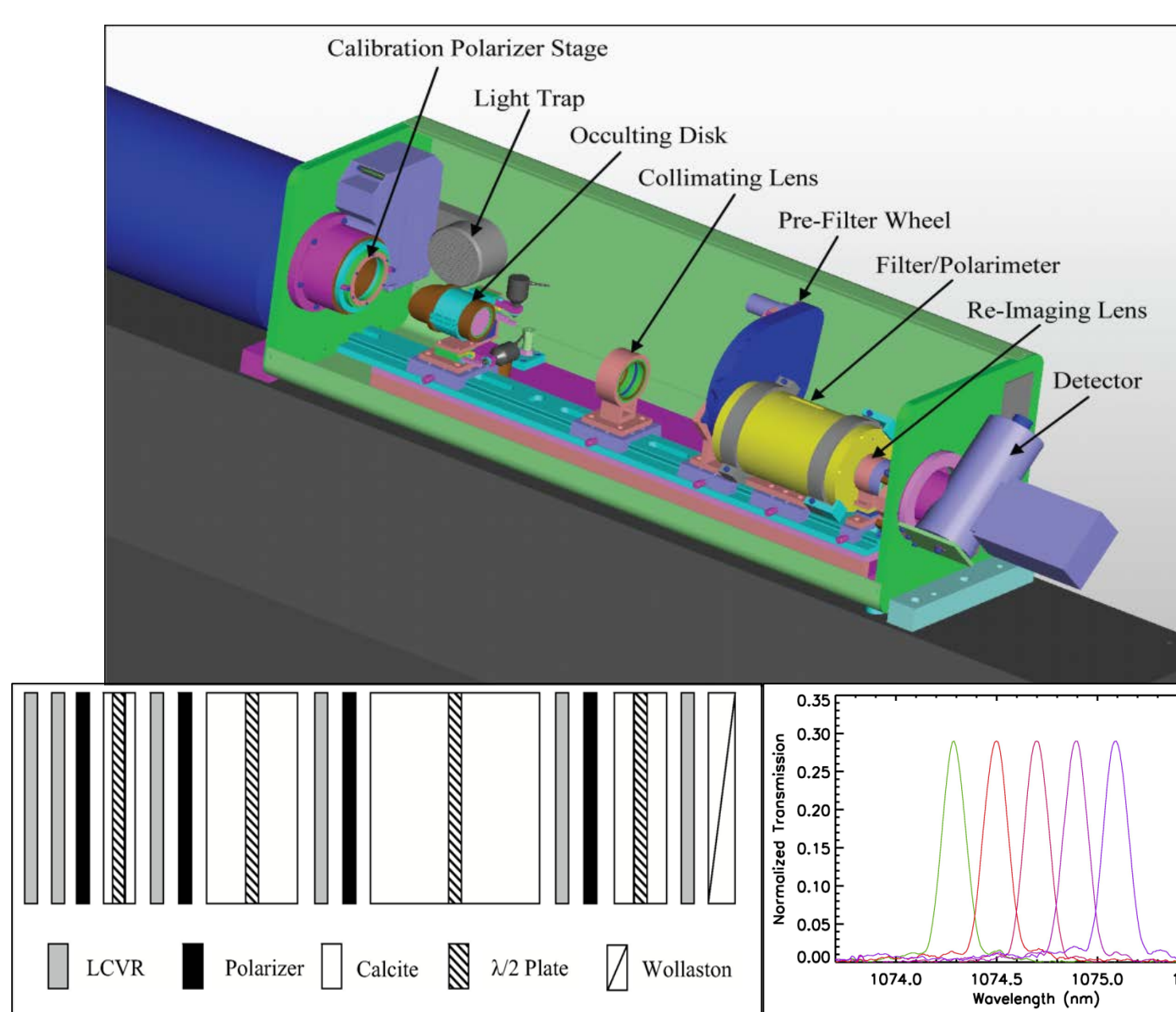
### Observational Requirements

Science Objective	FoV/Spatial Resolution	Physical Observable
1. Fast/Slow Wind, Coronal B structure	1.02-1.8 $R_{\odot}/1.5''$ pix. 1.02-2.8 $R_{\odot}/4.5''$ pix.	Waves; Doppler velocity, B-field direction, plasma density
2. Prominences, flux ropes	1.02-1.8 $R_{\odot}/1.5''$ pix.	B-field magnitude & direction from He I and Fe XIII
3. CME Shocks	1.02-2.8 $R_{\odot}/4.5''$ pix.	B-field magnitude & direction, plasma density; Waves; Doppler velocity.
4. Reconnection	1.02-1.8 $R_{\odot}/1.5''$ pix.	B-field magnitude & direction; Waves; Doppler velocity, plasma density

### Key Observables

Observable	Method of Analysis	Physical Process
Line-of-Sight B Field Strength	Circular Polarization	Long. Zeeman Effect
Plane-of-Sky B Field Direction	Linear Polarization	Resonance Scattering Effect (Hanle)
Line-of-Sight Velocity	Intensity vs. Wavelength	Doppler Effect
Plasma Density	Fe XIII 1074.7nm/1079.8nm Intensity Ratio, K-corona from continuum	Atomic Physics, Radiation Transfer

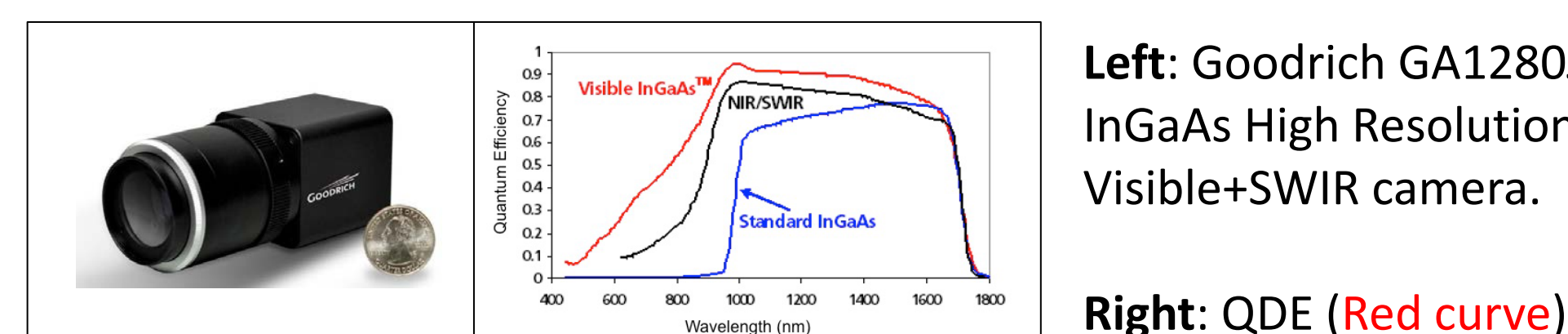
## 5. Instrument Design has Strong Heritage from CoMP



**Top:** A diagram showing the components of the existing Coronal Multi-channel Polarimeter (CoMP) currently operating at MLSO. **Bottom Left:** CoMP filter/polarimeter optical design. For WAMIS, the LCVRs will be replaced by FLCs and the Wollaston beam splitter (for line and continuum outputs) is not needed for WAMIS. **Bottom Right:** Transmission profiles for 5 tunings of CoMP near the Fe XIII 1074.7 nm line.

## 6. WAMIS Coronagraph and Detector System

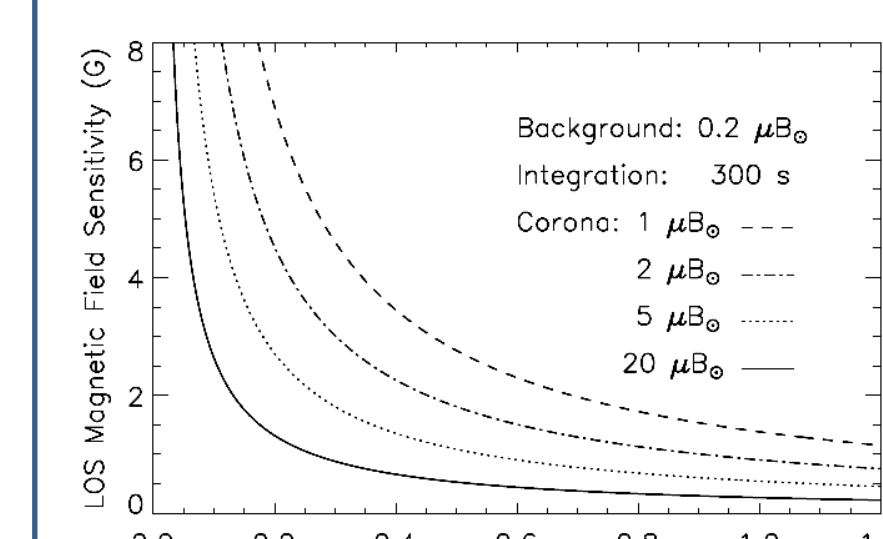
Table 4. Optical Design	
Objective	203.3cm fl.
Field Lens	31.0cm fl.
Collimating Lens	38.0cm fl.
Re-imaging Lens	High Mag. 38.0cm fl. Low Mag. 12.9cm fl.



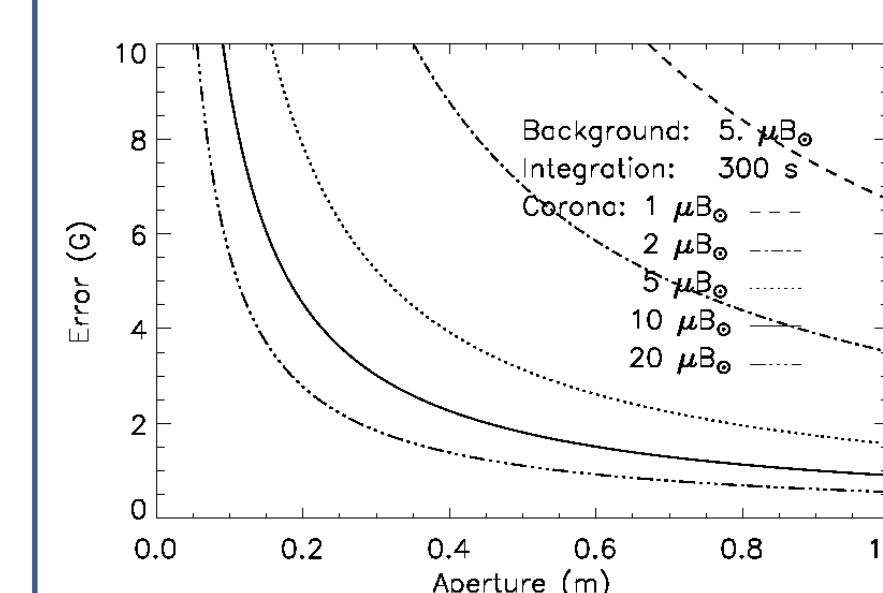
### Design Improvements beyond CoMP

- CoMP-S filter/polarimeter design will have **wider wavelength range** (See Section 3 above) enabling diagnostics at a range of temperatures.
- **Ferroelectric Liquid Crystals (FLCs)** will have a faster response time than the current Liquid Crystal Variable Retarders (LCVRs) on CoMP.
- Reduced atmospheric variations means that a beam splitter is not needed (spectral lines can be acquired with **higher spatial resolution**).
- f# can be optimized with **minimum instrumental polarization**.

## 7. Magnetic Field Measurement Sensitivity



B-field sensitivity vs. aperture for different coronal intensities ( $B_{\odot}$  is mean disk brightness). **WAMIS is sensitive to 2 G fields with a 20 cm aperture.** A background (instr. stray light level) of  $0.2\mu B_{\odot}$  is assumed.



On the contrary, on the ground (at MLSO) where typical background stray light levels are higher, a 20 cm instrument would have a sensitivity of only 4.5 G. It would take 5x longer to achieve a 2 G sensitivity on the ground.

**Note:** Wave observations (unpolarized) do not need the same accumulated exposure time for a given S/N and so an image cadence as short as 2 seconds can be achieved during the post-flight analysis of the same observing programs used for the magnetic field measurements.